Assessment of ground-based atmospheric observations for verification of greenhouse gas emissions from an urban region

Kathryn McKain[a,1], Steven C. Wofsy[a], Thomas Nehrkorn[b], Janusz Eluszkiewicz[b], James R. Ehleringer[c], and Britton B. Stephens[d]

[a]Department of Earth and Planetary Sciences, Harvard University, Cambridge, MA 02138; [b]Atmospheric and Environmental Research, Inc., Lexington, MA 02421; [c]Department of Biology, University of Utah, Salt Lake City, UT 84112; and [d]National Center for Atmospheric Research, Boulder, CO 80307

Edited by Mark H. Thiemens, University of California at San Diego, La Jolla, CA, and approved March 28, 2012 (received for review October 18, 2011)

International agreements to limit greenhouse gas emissions require verification to ensure that they are effective and fair. Verification based on direct observation of atmospheric greenhouse gas concentrations will be necessary to demonstrate that estimated emission reductions have been actualized in the atmosphere. Here we assess the capability of ground-based observations and a high-resolution (1.3 km) mesoscale atmospheric transport model to determine a change in greenhouse gas emissions over time from a metropolitan region. We test the method with observations from a network of CO_2 surface monitors in Salt Lake City. Many features of the CO_2 data were simulated with excellent fidelity, although data-model mismatches occurred on hourly timescales due to inadequate simulation of shallow circulations and the precise timing of boundary-layer stratification and destratification. Using two optimization procedures, monthly regional fluxes were constrained to sufficient precision to detect an increase or decrease in emissions of approximately 15% at the 95% confidence level. We argue that integrated column measurements of the urban dome of CO_2 from the ground and/or space are less sensitive than surface point measurements to the redistribution of emitted CO_2 by small-scale processes and thus may allow for more precise trend detection of emissions from urban regions.

atmospheric inversion | cities | climate change policy

Agreements to limit anthropogenic greenhouse gas (GHG) emissions will have major economic and political consequences. Compliance will be demonstrated primarily with self-reported emission inventories derived from activity data and generalized conversion factors (1, 2), but associated uncertainties may exceed the magnitude of emission reduction targets (2–5). Therefore, measurement, reporting, and verification (MRV) will be critical elements of any international climate treaty, as emphasized by a recent National Research Council (NRC) report (2), a related study by the JASON scientific advisory group (6), and by the Intergovernmental Panel on Climate Change (1). Verification procedures based on direct atmospheric observations can provide independent constraints on reported emissions and are necessary to ensure that emission reductions are actualized in the atmosphere.

The NRC report on MRV (2) highlighted the potential utility of atmospheric observations and models for detecting trends in emissions from strong localized source regions, such as urban areas, where enhancements in GHG concentration are readily detectable in the atmosphere. A large fraction of a country's emissions likely emanate from such regions and results from several representative cities over time could provide strong tests of claimed emission reductions at national or regional scales. But the NRC (2) estimated that current uncertainties in this approach exceed 100%, far too large to detect emission changes mandated by treaties or national policies. This imprecision is attributable to a dearth of research on the concept and the committee (2) speculated that near-term efforts could lead to substantial improvements, perhaps allowing for the detection of a change in emissions of 10–25% in 1 y and of 10% or less over 10 y.

The present study addresses the problem posed by the NRC (2) by assessing the current capability for using atmospheric observations to determine trends in GHG emissions at the scale of an urban region. We develop a high-resolution, urban-scale, observation-model framework, whereby observed GHG concentrations and presumed emissions are quantitatively related with an atmospheric transport and dispersion model (ATDM), and regional surface fluxes are estimated via an optimization procedure (7). Input data consist of measurements that define atmospheric concentration enhancements relative to air advected from outside the source region, plus an emissions inventory that prescribes the presumed spatial and temporal distributions of surface fluxes.

We apply the observation-model framework to a test case of Salt Lake City (SLC), leveraging a unique, long-term, publicly available dataset of urban atmospheric carbon dioxide (CO_2) concentrations (http://co2.utah.edu). We quantify the precision of the method for detecting changes in monthly emissions from this urban region, and assess how statistical properties of urban CO_2 concentrations and features of current state-of-the-art models limit trend detection capabilities. Finally, we suggest how the framework might be improved, through both alternative measurement strategies and enhanced model capabilities.

Previous Studies of Urban CO_2

Many studies (e.g., refs. 8–10) have described near-surface CO_2 concentrations and fluxes in a variety of urban environments and attributed observed variability to both atmospheric dynamics and local emission patterns. City-scale fluxes have been derived with mass-balance approaches using surface data from Krakow (11) and aircraft data from Indianapolis (12). Ratios of carbon monoxide (CO) and CO_2 from a site near Beijing were used to define trends in combustion efficiency (13). None of the approaches taken in these studies are capable of quantifying trends in emissions at the full urban scale and with the accuracy required for verification.

Levin et al. (14) presented the only prior study to accurately assess emission inventories over time at a regional scale, using a multidecadal dataset of atmospheric GHG concentrations, $^{14}CO_2$, and radon-222 from Heidelberg. Unfortunately, the key element of this unique study (long-term, high-frequency, radio-

Author contributions: S.C.W. and T.N. designed research; K.M., T.N., J.E., J.R.E., and B.B.S. performed research; T.N. and J.E. adapted the WRF-STILT model to the study; J.R.E. and B.B.S. collected atmospheric data; K.M. and S.C.W. analyzed data; and K.M. and S.C.W. wrote the paper.

The authors declare no conflict of interest.

This article is a PNAS Direct Submission.

Freely available online through the PNAS open access option.

[1]To whom correspondence should be addressed. E-mail: kmckain@fas.harvard.edu.

This article contains supporting information online at www.pnas.org/lookup/suppl/doi:10.1073/pnas.1116645109/-/DCSupplemental.

isotope measurements) are not currently widely reproducible due to cost and technological requirements. The framework described below uses measurements made by readily available sensors combined with open-source meteorological data and models, and is thus scalable to numerous locations, as needed for MRV.

Characterization of CO_2 Observations from Salt Lake City

The SLC CO_2 measurement program was initiated as part of a study of carbon and oxygen isotopes focused on urban source attribution. Pataki et al. (15–17) estimated the proportional contributions of natural gas versus gasoline combustion and biological respiration to observed CO_2 enhancements, and (18) suggested the application of CO_2 as a tracer of atmospheric transport and mixing in complex terrain. Pataki et al. (19) found general agreement between SLC eddy-flux measurements and an emissions inventory compiled for the upwind area. SLC CO_2 was simulated with a multiple box model to understand the relative contributions of meteorology and anthropogenic and biological surface fluxes to observed daily and seasonal cycles (20).

The SLC CO_2 data follow a distinctive diel pattern, in which concentrations are higher at night and lower during the day (Fig. 1*A*), following the daily cycle of the mixing height, which is shallow at night due to thermal stratification, and deep most days due to solar heating of the surface. The diel cycle of CO_2 concentrations is notably out of phase with emissions (Fig. 1*B*), implying that thermally forced circulations impose a stronger influence on near-surface concentrations than emission rates (20). Mean hourly enhancements over background in 2006 at the downtown site ranged from approximately 0–20 ppm ($1\sigma \cong 16$ ppm) in the afternoon (12–18 h mountain standard time, MST) and from approximately 20–60 ppm ($1\sigma \cong 35$ ppm) at night (22-04 h MST). Peak concentrations are typically observed in the early morning due to the combined effects of atmospheric stratification and increased emissions from rush-hour traffic; concentrations drop rapidly thereafter with the onset of deeper vertical mixing in midmorning (20) (Fig. 1*A*).

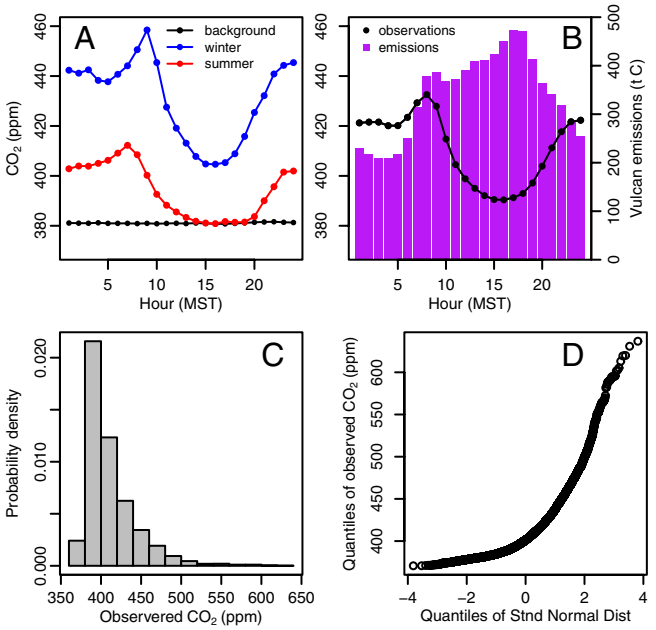

Fig. 1. Average hourly observed CO_2 concentration at the downtown site in 2006. (*A*) Averaged by hour of the day from winter (Dec.–Feb.) and summer (June–Aug.) months, and from nearly the entire year (April–Dec.) at the background site. (*B*) Observed CO_2 from the whole year (*Left y* axis) versus average hourly CO_2 emissions estimated from the Vulcan inventory for a 0.5° × 0.5° area encompassing the Salt Lake Valley (*Right y* axis). (*C* and *D*) Distribution of observed CO_2.

Seasonal averages are lower in summer than winter (Fig. 1*A*). During the growing season, CO_2 concentrations sometimes fall below background in the afternoon, likely due to uptake by urban trees (21). In the winter, the Salt Lake Valley (SLV) is prone to atmospheric temperature inversions, which suppress vertical mixing and give rise to sustained periods of elevated concentrations. The overall distribution of observed CO_2 is heavily right-skewed (Fig. 1*C*) and is seemingly comprised of two subpopulations, representing stratified and unstratified conditions (Fig. 1*D*).

Simulation of CO_2 Observations

We used the Weather Research and Forecasting—Stochastic Time-Inverted Lagrangian Transport (WRF-STILT) atmospheric transport model (http://stilt-model.org) and antropogenic and biogenic flux inventories to simulate the SLC CO_2 data, as described in *Materials and Methods* and references therein. The observation-model framework was tested for four monthly time periods from different seasons in 2006 (Table 1) and three sampling locations in SLC. We assessed two horizontal resolutions of the ATDM, 4 km ("baseline") and 1.3 km ("high-resolution") (Fig. S1), the latter of which was tested for only a 2-wk subset of the autumn time period. The high-resolution ATDM included parameterization of an urban canopy model (UCM) (22), which allows for greater heterogeneity in surface properties related to the urban environment than is available in standard WRF configurations. Fig. 2 shows hourly observed and simulated CO_2 for baseline and high-resolution models. The time series demonstrates the model's general capability for capturing the typical diel pattern of near-surface CO_2 concentrations, albeit with a systematic underestimation using a priori emissions (Fig. 2*B*).

Elsewhere (23), we evaluated the performance of the two WRF configurations (baseline and high-resolution with an UCM) by comparing observed and modeled meteorological parameters from the SLV. The high-resolution meteorological configuration with the UCM led to improved representation of the daily evolution of the surface (2 m) temperature and boundary-layer height, especially when the flow was driven by local circulations. Likewise, the high-resolution WRF-STILT model resulted in changes in simulated CO_2, in particular related to the timing of the nocturnal boundary-layer formation and breakup (Fig. 2*B*).

The model captures many weather-related events such as the multiday persistence of low concentrations around October 16 and August 30 (Fig. 2*A* and Fig. S2*B*). Some, generally short, time periods are poorly simulated, such as on June 24–25, when the model substantially underestimates observed CO_2 (Fig. S2*A*). The model also captures seasonal variability in the magnitude and variance of CO_2 enhancements (Table 1). In December, the model is often unable to simulate CO_2 concentrations at hourly resolution (Fig. S2*D*), although this result was not unexpected because meteorological conditions during strong winter temperature inversions in valleys are difficult to simulate (24). But the model does capture the very high variances in CO_2 and the general amplitude of enhancements over background during December (Table 1 and Fig. S2*D*).

The model biosphere sometimes draws down simulated CO_2 in SLC below background during midday, in the spring and summer months only, in agreement with the observations (Fig. 1*A*) and

Table 1. Means and standard deviations (1σ) of hourly observed and baseline modeled CO_2 (ppm) at the downtown site for the four simulated time periods from 2006

Time period	Sample size	Mean (SD)	
		Observed	Modeled
June 13–27	334	397 (14)	391 (13)
Aug. 23–Sep. 14	545	395 (17)	393 (19)
Oct. 10–29	461	422 (34)	405 (26)
Nov. 29–Dec. 31	785	439 (47)	429 (46)

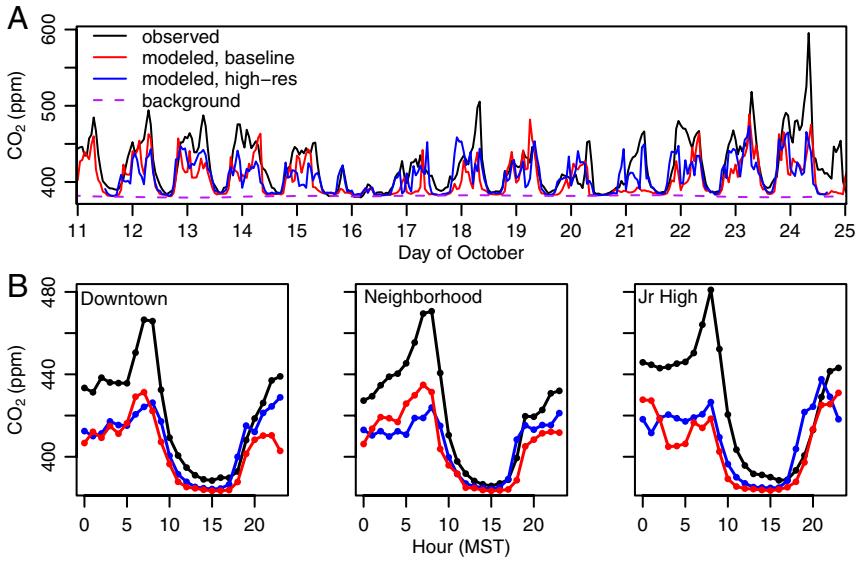

Fig. 2. Hourly observed and modeled CO_2 concentrations for two weeks in October 2006 (*A*) at the downtown site, and (*B*) averaged by hour of the day at the downtown, neighborhood, and junior high sites.

known irrigation practices, and contributes small enhancements from plant and soil respiration during all other times. Overall, the model suggests that the biosphere has a relatively minor influence on CO_2 concentrations in SLC, which is not surprising given the semiarid ecosystems of the region and previous findings (19–21).

Quantification of the Data-Model Relationship

Two approaches were employed to quantify the relationships between hourly observed and simulated CO_2 concentrations for the four time periods and three observation sites. We first applied a type II, standard major axis regression (25) to fit a line to observed versus simulated values (Fig. 3). The inverse of the regression line slope provides an estimate of the optimum factor by which to scale the emissions inventory to best match the observed data. Confidence intervals (CIs) on the slope define our ability to detect changes in emissions over time at the 95% confidence level, assuming spatial and temporal biases in the model are unchanging over time.

Because the regression is based on modeled and observed values paired in time, it may be susceptible to sporadic failures in the transport model, and thus may lead to CIs which are overly pessimistic in terms of trend detection capability. We therefore adopted an alternative approach which gives less weight to poorly timed events by selecting scaling factors that minimize the differences in observed and simulated population means from each site and time period. Ninety-five percent CIs for this optimization procedure were calculated using a percentile bootstrap.

Table 2 gives scaling factors generated by both optimization methods for the high-resolution and baseline models for October. Table S1 gives scaling factors for the other time periods. Mean scaling factors for October from the high-resolution model are between 1.5 and 1.8, with 95% CIs that are ±7–8% of the mean (Table 2). Mean scaling factors for other seasons from the base-

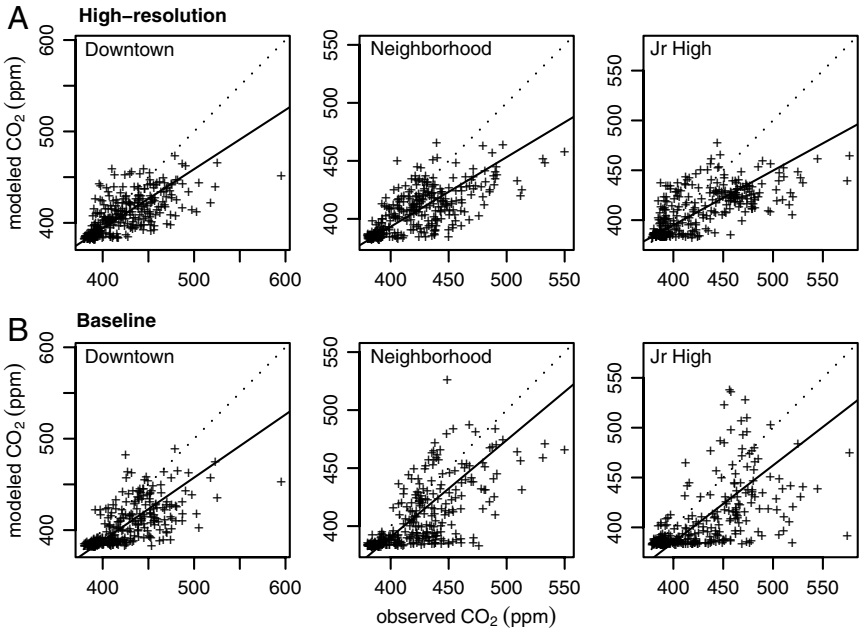

Fig. 3. Hourly modeled versus observed CO_2 at three sites for a two-week time period in October 2006 resulting from (*A*) high-resolution and (*B*) baseline model configurations. Solid lines are standard major axis regression lines and dashed lines are one-to-one shown for reference.

Table 2. Mean scaling factors by two optimization procedures and 95% confidence intervals for baseline and high-resolution models at three sites for a 2-wk time period in October 2006

Site	Model configuration	Scaling factor (±95% CI) (CI/mean)	
		by regression	by minimizing differences in means
Downtown	high-res, UCM	1.54 (±0.12) (±8%)	1.52 (±0.11) (±7%)
	baseline	1.45 (±0.12) (±8%)	1.83 (±0.16) (±9%)
Neighborhood	high-res, UCM	1.67 (±0.13) (±8%)	1.63 (±0.11) (±7%)
	baseline	1.20 (±0.10) (±8%)	1.67 (±0.16) (±9%)
Junior high	high-res, UCM	1.83 (±0.15) (±8%)	1.59 (±0.12) (±8%)
	baseline	1.30 (±0.11) (±9%)	1.93 (±0.24) (±12%)

$N = 317$. Scaling factors were generated as the inverse of standard major axis regression line slopes and by minimizing the difference in observed and simulated sample means. Confidence interval half-widths are also expressed as percent deviations from the means.

line model mostly range between 1 and 2 and have 95% CIs that are ±6–13% of the means (Table S1).

Scaling factors for the high-resolution model are similar to those for the baseline model, but are more consistent between sites and optimization methods, and have narrower CIs (Table 2). We infer that the high-resolution model is better for trend assessment, although this was not immediately apparent by visual inspection of Fig. 2. Improvements by the high-resolution model are especially noticeable in the decreased persistence of very low model values when the data indicate elevated concentrations (Fig. 3). When inventory fluxes are multiplied by the optimal scaling factors, the distributions of simulated CO_2 from the high-resolution model are remarkably close to observed distributions (Fig. 4), although variance was not included in the optimization procedure.

These results support the application of high-resolution modeling, and optimization of sample distributions and regressions, for determining trends in urban emissions. We infer from the results reported in Table 2 for the high-resolution model that 15% is a conservative estimate of the minimum increase or decrease in monthly emissions detectable by our observation-model framework, although caution must be exercised in generalizing these results due to the short time period (approximately 2 wk) for which the high-resolution model was tested. By applying the framework to several years' worth of data, changes in scaling factors, and thus relative changes in emissions, could likely be estimated with greater precision.

The scaling factors generated in this study are significantly greater than the expected value of 1.0 (Table 2 and Table S1), implying that emissions were underreported for the SLC urban core and/or that modeled meteorology was too well-mixed. However, absolute emissions cannot be evaluated with the same level of accuracy as can a change in emissions over time because our statistical procedures do not account for systematic model errors, such as possible over- or underestimation of the mean boundary-layer height or biases in the presumed spatial distribution of emissions. To evaluate absolute emissions, rather than a change in emissions, a fiducial tracer or a sustained release experiment would be necessary.

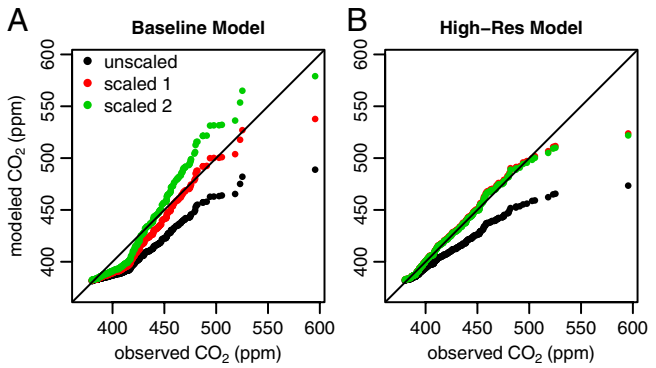

Fig. 4. Quantile–quantile plots of hourly modeled versus observed CO_2 at the downtown site for two-weeks in October 2006 from (*A*) baseline and (*B*) high-resolution models. Model values unscaled and scaled by the two optimization methods are shown. For the high-resolution model, scaling factors by the two optimization methods are near identical, so the two scaled model distributions are nearly indistinguishable.

Approaches for Improving Emission Trend Detection

A key limitation to further constraining emissions is the inability of current models to simulate small-scale atmospheric processes. Examples of processes which affect concentrations over short timescales at individual urban sites, but which models cannot explicitly represent, include circulations at building, street, and neighborhood scales, and intermittent turbulence in the nocturnal boundary layer. Improved parameterization of these processes could significantly improve the capability of atmospheric models to simulate urban GHG concentrations. Representation of proximal emission processes at an enhanced spatial resolution similar to that of the meteorology (1.3 km) could also lead to improved simulations.

Contrary to the expectations of some (cf. ref. 6), the SLC case suggests that increasing the number of surface measurement stations across the city would be ineffective at substantially improving the observational approach for detecting a change in emissions. Simulations indicate that individual measurements sites are sensitive to emissions across the full urban region (Fig. S3). Observed CO_2 concentrations at the five measurement stations in SLC are strongly correlated on a daily basis (Fig. S4) because within day variance is dominated by the diel cycles in atmospheric stability (Fig. 1) and forcing of these cycles occurs on the scale of the whole valley. This finding suggests that the current network of five stations in SLC is more than adequate for characterizing the daily cycle of urban-scale CO_2. If we consider just the afternoon hours, the opposite problem occurs: Fluctuations at stations quite close together (<5 km) are not significantly correlated (Fig. S4), suggesting that small-scale processes are responsible for CO_2 concentration variations in the afternoon and are not directly tied to region-wide emissions. Hence, denser measurements of such variations would not help to significantly improve determination of regional trends.

Alternative measurement strategies that are less sensitive to the details of atmospheric circulation and emissions may lead to improved trend detection capability. Shallow circulations rearrange CO_2 between sublayers of the atmosphere on hourly timescales, but for the duration that emitted CO_2 remains in the urban region, total column amounts are directly linked to total emissions. Fig. 5 shows simulations of the characteristic pattern of CO_2 enhancement, vertically integrated through the partial atmospheric column, which comprises the "urban dome" over the SLV. Observations throughout the column are not available for validation, but simulations appear to have sufficient fidelity at the surface (Fig. 2) to justify exploration of the character of the urban dome through modeling. The position of the urban dome shifts with the wind, but, due to the valley topography (Fig. 5*C*

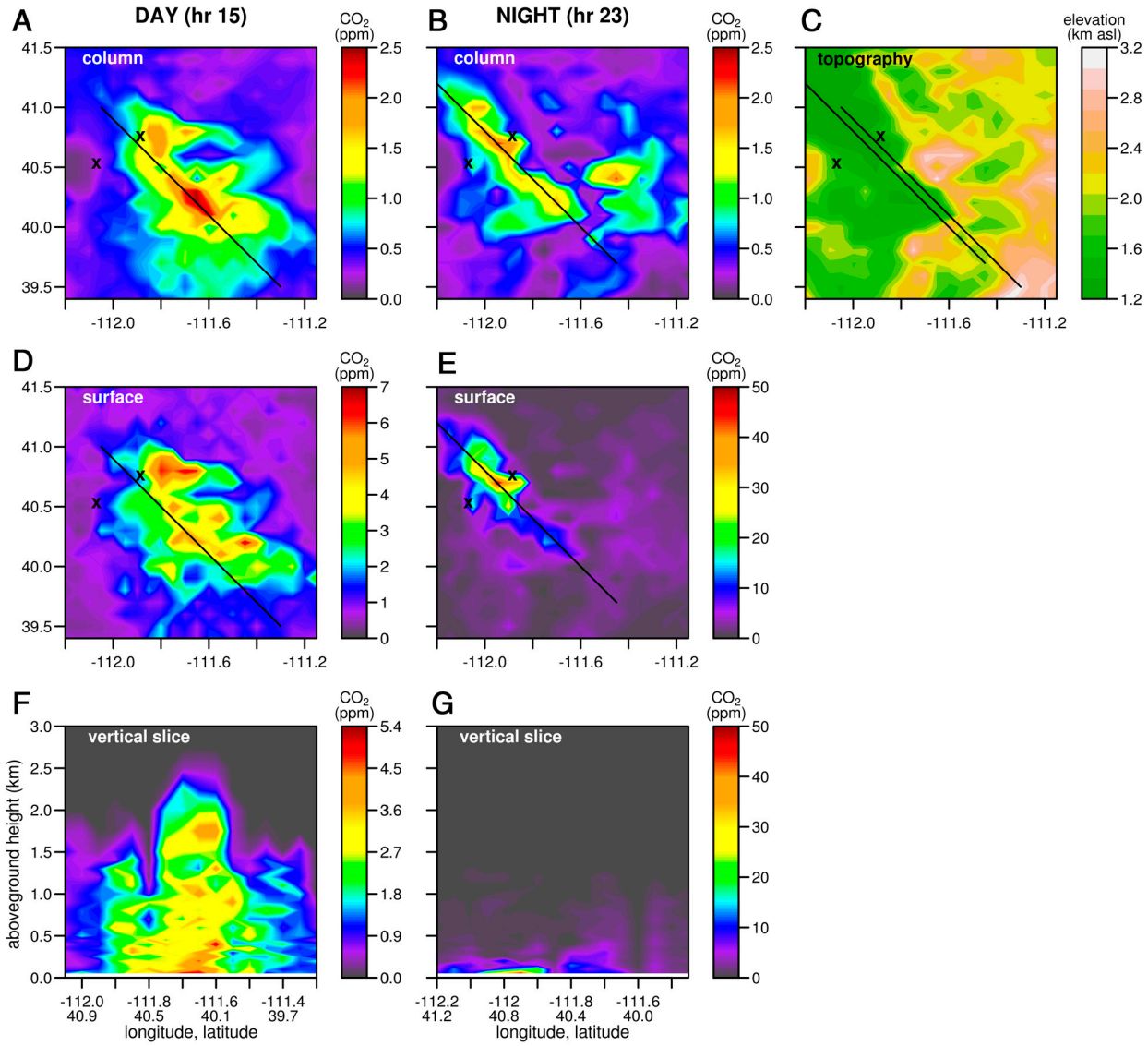

Fig. 5. Simulated partial column-averaged XCO_2 (ppm) enhancements above background up to 3 km above SLC and the surrounding area on October 18, 2006 at 15 h (*A*) and 23 h (*B*) MST. (*D* and *E*) Simulated CO_2 enhancement near the surface, 50 m above the ground, for the same times and locations as in *A* and *B*. (*F* and *G*) Vertical slices through the areas of maximum XCO_2 enhancement in the urban domes. (*C*) Topography in kilometers above sea level. The downtown and rural measurement sites are marked with Xs for reference. Lines in *A*–*E* show the positions of the transects plotted in *F* and *G*. Note that the two upper-left panels have the same scale, but the four lower panels do not.

and Fig. S5), its core generally lies on a predictable NW–SE axis. During the day, the dome extends vertically up to 2 km, but at night, excess CO_2 is contained within a thin layer less than 100-m deep (Fig. 5 *F* and *G*).

The differences between enhancements at the surface and those integrated through the column are striking. The areal extent and magnitude of column enhancements are larger in the day than the night (Fig. 5 *A* and *B*), directly reflecting the higher daytime emissions (Fig. 1*B*) that we wish to measure. We infer that urban enhancements in column amounts are more sensitive to regional-scale meteorology, especially mean wind speeds, and to emissions integrated through the whole urban region. Conversely, surface values are more sensitive to boundary-layer height, shallow circulations, and local traffic emissions. Mean winds are much easier to model than boundary-layer heights, and can be validated with hourly observations from airports and weather stations. Broad-scale emission inventories are better defined than fine-scale, day-to-day traffic patterns.

The magnitude of the anthropogenic CO_2 enhancement in the partial column integral is notably smaller than at the surface, by factors of 2 (daytime, Fig. 5 *A* and *D*) to 20 (nighttime, Fig. 5 *B* and *E*), suggesting that increased accuracy may be required to both measure and simulate the column enhancement. To our knowledge, ground-based measurements of CO_2 column amounts with the accuracy required for verification have been demonstrated just once, in Los Angeles, where peak concentrations in the column were indeed observed in midday (26). Total column measurements could be made from space, obviating the need for many surface stations and eliminating intrusive measurements on the territory of a treaty signatory. The widespread, spatially heterogeneous, and shifting nature of the simulated SLC urban dome suggests that remote sensing of the dome may offer the best route for its full characterization. Unfortunately, no presently planned satellite has the necessary orbit or targeting capability.

Summary and Future Directions

We have demonstrated an observation-model framework capable of detecting a change in anthropogenic CO_2 emissions of 15% or more from an urban region on a monthly basis. The model framework consists of an atmospheric transport model (STILT) driven

by a high-resolution (1.3 km) mesoscale meteorological model (WRF) and coupled to moderately high-resolution models of the spatial and temporal distribution of anthropogenic emissions (Vulcan) and biogenic fluxes. We compared simulations to observations from four time periods and three locations in SLC. Constraints on emission rates were obtained by optimizing the emission model two ways, both of which gave similar central values and confidence intervals.

The observation-model framework is readily scalable to other sites using commercial sensors and open-source models. Measurements are needed to define background (upwind) values, especially for urban areas downwind of other major source regions. For heavily vegetated cities, it will be necessary to distinguish anthropogenic from biogenic emissions, possibly with tracer measurements of fossil fuel combustion (e.g., CO, ^{14}C). Analysis of the statistical correlations among the SLC measurement sites indicates that five was an ample number, although this result likely depends on SLC's relatively small size and topographic confinement.

We argue that measurements of vertically integrated column amounts would provide more new information than would additional surface sites. In our estimation, column measurements offer a promising route for improved detection of CO_2 emissions from major source regions, complementing or possibly obviating the need for extensive surface measurements near these areas. Remote sensing of the column-integrated urban dome appears to offer the best route for accurate verification of emission inventories of CO_2 and other GHGs.

Materials and Methods

Observations. A network of CO_2 measurement sites has been operated at up to five locations in SLC and its suburbs (Fig. S5 and Table S2) since 2001. We modeled CO_2 data from 2006 because of the quality and consistency of the data from that year. For this study, we focused on modeling observations from the downtown, neighborhood, and junior high sites (Fig. S5 and Table S2). Two-day moving averaged CO_2 concentrations (Fig. S6) from the Hidden Peak mountaintop site (http://raccoon.ucar.edu) outside SLC were used to represent the background CO_2 concentration in air coming in to the city (*SI Materials and Methods*).

CO_2 Flux Fields. The Vulcan database (v2.0) (http://vulcan.project.asu.edu) (27) was used for an anthropogenic CO_2 emissions field. Vulcan provides estimates of CO_2 emissions due to fossil fuel combustion from each of eight economic sectors for the United States in 2002 as a gridded product with a time and space resolution of 1 h and 0.1°, respectively. According to Vulcan, the major anthropogenic CO_2 sources in the SLV are from the transportation, residential, and industrial sectors (Fig. S7). To minimize the inclusion of year-specific emissions information while still retaining hour-of-the-day and day-of-the-week signatures, we averaged the Vulcan database by month, day-of-week, and hour-of-the-day (Fig. S7) prior to integrating it into the modeling framework. It was not necessary to scale the inventory to 2006, the year of interest for our study, because the observation-model framework is intended to determine a change in emissions over time, but not to evaluate absolute emissions from any single time period. CO_2 fluxes due to photosynthetic uptake and soil and plant respiration were represented with a simple biosphere model, which is described in *SI Materials and Methods* and Table S3.

Atmospheric Transport Model. The STILT model (28) was used as the ATDM. The STILT model was driven with customized meteorological fields from the advanced research version of the WRF (v3.2) model (29, 30). Meteorological fields were generated at three gridded resolutions (4, 12, and 36 km) in a nested arrangement centered on SLC (Fig. S1) for four approximately monthly time periods (Table 1). A set of high-resolution (1.3 km for the inner nest) WRF (v3.2.1) fields with an UCM parameterization (22) were generated for a 2-wk subsample of the October time period. See *SI Materials and Methods* for further details on the modeling framework.

ACKNOWLEDGMENTS. We thank Dean Cardinale and the Snowbird Ski and Summer Resort for their support at Hidden Peak (HDP), and Kevin Gurney for providing the Vulcan emission inventory. This study was supported by Grants NNX11AG47G and NNX08AR47G from the National Aeronautics and Space Administration and ATM-0830916 from the National Science Foundation (NSF) to Harvard University, by NSF Grant ATM-0836153, to Atmospheric and Environmental Research, Inc., and by the US intelligence community. The SLV CO_2 observation network was supported by the Office of Science (Biological and Environmental Research), US Department of Energy, Grants DE-FG02-06ER64309 and DESC0005266. HDP measurements were supported by NSF Grant EAR-0321918 and National Oceanic and Atmospheric Administration Grant NA09OAR4310064. The National Center for Atmospheric Research is sponsored by the NSF.

1. Eggleston HS, Buendia L, Miwa K, Ngara T, Tanabe K, eds. (2006) 2006 IPCC Guidelines for National Greenhouse Gas Inventories. (Inst for Global Environmental Strategies, Hayama, Japan), prepared by the National Greenhouse Gas Inventories Program.
2. Committee on Methods for Estimating Greenhouse Gas Emissions (2010) Verifying greenhouse gas emissions: method to support international climate agreements, National Research Council. (Natl Acad Press, Washington, DC).
3. Gregg JS, Andres RJ, Marland G (2008) China: Emissions pattern of the world leader in CO_2 emissions from fossil fuel consumption and cement production. *Geophys Res Lett* 35:L08806.
4. Peylin P, et al. (2011) Importance of fossil fuel emission uncertainties over Europe for CO_2 modeling: Model intercomparison. *Atmos Chem Phys* 11:6607–6622.
5. Marland G (2008) Uncertainties in accounting for CO_2 from fossil fuels. *J Ind Ecol* 12:136–139.
6. JASON (2011) Methods for remote determination of CO_2 emissions. (MITRE Corp, McLean, VA), JSR-10-300; www.fas.org/irp/agency/dod/jason/emissions.pdf.
7. Ciais P, et al. (2010) Atmospheric inversions for estimating CO_2 fluxes: Methods and perspectives. *Clim Change* 103:69–92.
8. McRae JE, Graedel TE (1979) Carbon dioxide in the urban atmosphere: Dependencies and trends. *J Geophys Res* 84:5011–5017.
9. Bergeron O, Strachan IB (2011) CO_2 sources and sinks in urban and suburban areas of a northern mid-latitude city. *Atmos Environ* 45:1564–1573.
10. Gratani L, Varone L (2005) Daily and seasonal variation of CO_2 in the city of Rome in relationship with traffic volume. *Atmos Environ* 39:2619–2624.
11. Zimnoch M, Godlowska J, Nick JM, Rozanski K (2010) Assessing surface fluxes of CO_2 and CH_4 in urban environment: A reconnaissance study in Krakow, southern Poland. *Tellus B* 62:573–580.
12. Mays KL, et al. (2009) Aircraft-based measurements of the carbon footprint of Indianapolis. *Environ Sci Technol* 43:7816–7823.
13. Wang Y, et al. (2010) CO_2 and its correlation with CO at a rural site near Beijing: implications for combustion efficiency in China. *Atmos Chem Phys* 10:8881–8897.
14. Levin I, Hammer S, Eichelmann E, Vogel FR (2011) Verification of greenhouse gas emission reductions: The prospect of atmospheric monitoring in polluted areas. *Philos Trans R Soc A* 369:1906–1924.
15. Pataki DE, Bowling DR, Ehleringer JR (2003) Seasonal cycle of carbon dioxide and its isotopic composition in an urban atmosphere: Anthropogenic and biogenic effects. *J Geophys Res* 108:4735.
16. Pataki DE, Bowling DR, Ehleringer JR, Zobitz JM (2006) High resolution atmospheric monitoring of urban carbon dioxide sources. *Geophys Res Lett* 33:L038143.
17. Pataki DE, Xu T, Luo YQ, Ehleringer JR (2007) Inferring biogenic and anthropogenic carbon dioxide sources across an urban to rural gradient. *Oecologia* 152:307–322.
18. Pataki DE, et al. (2005) Can carbon dioxide be used as a tracer of urban atmospheric transport? *J Geophys Res* 110:D15102.
19. Pataki DE, et al. (2009) An integrated approach to improving fossil fuel emissions scenarios with urban ecosystem studies. *Ecol Complex* 6:1–14.
20. Strong C, Stwertka C, Bowling DR, Stephens BB, Ehleringer JR (2011) Urban carbon dioxide cycles within the Salt Lake Valley: A multiple-box model validated by observations. *J Geophys Res* 116:D15307.
21. Ramamurthy P, Pardyjak ER (2011) Toward understanding the behavior of carbon dioxide and surface energy fluxes in the urbanized semi-arid Salt Lake Valley, Utah, USA. *Atmos Environ* 45:73–84.
22. Chen F, et al. (2010) The integrated WRF/urban modeling system: Development, evaluation, and applications to urban environmental problems. *Int J Climatol* 31:273–288.
23. Nehrkorn T, et al. (2011) Modeling the urban circulation in the Salt Lake City area using the WRF urban canopy parameterization. Allwine-Doran Retrospective of the Special Symposium on Applications of Air Pollution Meteorology. (Am Meteorological Society, Boston, MA), http://ams.confex.com/ams/91Annual/webprogram/Paper186119.html.
24. Finn D, Clawson KL, Carter RG, Rich JD (2008) Plume dispersion anomalies in a nocturnal urban boundary layer in complex terrain. *J Appl Meteorol Clim* 47:2857–2878.
25. Warton DI, Wright IJ, Falster DS, Westoby M (2006) Bivariate line-fitting methods for allometry. *Biol Rev Cambridge Philos Soc* 81:259–291.
26. Wunch D, Wennberg PO, Toon GC, Keppel-Aleks G, Yavin YG (2009) Emissions of greenhouse gases from a North American megacity. *Geophys Res Lett* 36:L15810.
27. Gurney KR, et al. (2009) High resolution fossil fuel combustion CO_2 emission fluxes for the United States. *Environ Sci Technol* 43:5535–5541.
28. Lin JC, et al. (2003) A near-field tool or simulating the upstream influence of atmospheric observations: The Stochastic Time-Inverted Lagrangian Transport (STILT) model. *J Geophys Res* 108:4493–4510.
29. Skamarock WC, Klemp JB (2008) A time-split nonhydrostatic atmospheric model for weather research and forecasting applications. *J Comput Phys* 227:3465–3485.
30. Nehrkorn T, et al. (2010) Coupled weather research and forecasting-stochastic time-inverted lagrangian transport (WRF-STILT) model. *Meteorol Atmos Phys*, pp:51–64.